

FAST, HIGH-ACCURACY, RANDOMIZED NULLSPACE COMPUTATIONS FOR TALL MATRICES*

ETHAN N. EPPERLY[†], TAEJUN PARK[‡], AND YUJI NAKATSUKASA[§]

Abstract. In this paper, we develop RLOBPCG, an efficient method for computing a small number of singular triplets corresponding to the smallest singular values of large, tall matrices. The algorithm combines randomized preconditioner from the sketch-and-precondition techniques with the LOBPCG eigensolver: a small sketch is used to construct a high-quality preconditioner, and LOBPCG is run on the Gram matrix to refine the singular vector. Under the standard subspace embedding assumption and a modest singular value gap between the two smallest singular values, we prove that RLOBPCG converges geometrically to the minimum singular vector. In numerical experiments, RLOBPCG achieves near-optimal accuracy on matrices with up to 10^6 rows, outperforming classical LOBPCG and Lanczos methods by a speedup of up to $12\times$ and maintaining robustness when other iterative methods fail to converge.

Key words. singular vector, nullspace, LOBPCG, sketching, preconditioning

MSC codes. 65F15, 68W20, 65D15

1. Introduction. The singular vectors of a matrix $\mathbf{A} \in \mathbb{C}^{m \times n}$ are fundamental objects in matrix computations and data analysis. Much work has been dedicated to efficiently computing the *dominant* singular vectors, those associated with the largest singular values. The dominant singular values comprise the optimal low-rank approximation to \mathbf{A} , and computing them is necessary for applications in genetic data analysis [1], model reduction [3], compression of large data [46], and many other areas.

Computation of the *minimum singular vectors*, those with the smallest singular values, has received significantly less attention. In the case where \mathbf{A} is tall and rank-deficient, the minimum singular vectors span the *nullspace* of \mathbf{A} . When \mathbf{A} is not rank-deficient, the minimum singular vectors can be interpreted as spanning the *near-nullspace* of \mathbf{A} , the vectors that are amplified by \mathbf{A} the least. Minimum singular vector computations are used in applications spanning total least squares [18], rational approximation [31, 32], frequency estimation [40], computational topology [26], and multivariate polynomial root-finding [6, 20].

This paper focuses on computing a small number, say 1 to 10, of minimum singular vectors of a large, very tall matrix $\mathbf{A} \in \mathbb{C}^{m \times n}$, for which $m \gg n \gg 1$. Our approach combines the *randomized preconditioning* approach of Rokhlin & Tygert [38] (popularized as *Blendenpik* by [5]) with a preconditioned eigensolver such as LOBPCG [23]. This combination is simple and natural, but to the best of our knowledge, has not yet been proposed, analyzed, and tested. We call this procedure RLOBPCG. To compute a single minimum singular vector, RLOBPCG proceeds as follows:

1. **Generate embedding.** Draw a random embedding matrix (i.e., a “sketch-

*Date: February 20, 2026

Funding: The authors acknowledge support from the Miller Institute for Basic Research in Science, University of California Berkeley (ENE), the RandESC project funded by the Swiss Platform for Advanced Scientific Computing (TP), and EPSRC grants EP/Y010086/1 and EP/Y030990/1 (YN). ENE also received support, under aegis of Joel Tropp, by ONR grant N00014-24-1-2223 and the Caltech Carver Mead New Adventures Fund.

[†]Department of Mathematics, University of California Berkeley, Berkeley, CA 94720, USA (<https://ethanepperly.com>, epperly@berkeley.edu)

[‡]Institute of Mathematics, EPF Lausanne, 1015 Lausanne, Switzerland, (taejun.park@epfl.ch).

[§]Mathematical Institute, University of Oxford, Oxford, OX2 6GG, UK, (nakatsukasa@maths.ox.ac.uk).

- ing matrix") $\mathbf{S} \in \mathbb{C}^{d \times m}$ with $d = \mathcal{O}(n)$ or $d = \mathcal{O}(n \log n)$ rows.
2. **Sketch and factorize.** Compute the sketch $\mathbf{S}\mathbf{A}$ and form its (economy-size) decomposition $\mathbf{S}\mathbf{A} = \mathbf{U}\Sigma\mathbf{V}^*$. ($*$ denotes the conjugate transpose.)
 3. **Define preconditioner and initialization.** Set $\mathbf{P} := \mathbf{V}\Sigma^{-1}$ and $\mathbf{v}_0 = \mathbf{v}_{-1} := \mathbf{P}\mathbf{e}_n/\|\mathbf{P}\mathbf{e}_n\|$, where \mathbf{e}_n is the n th standard basis vector.¹
 4. **LOBPCG.** Apply LOBPCG to the Gram matrix $\mathbf{A}^*\mathbf{A}$ with preconditioner $\mathbf{P}\mathbf{P}^*$. For $i = 0, 1, 2, \dots$, do the following:

- (a) **Generate new search direction.** Set

$$(1.1) \quad \mathbf{w}_i := \mathbf{P}(\mathbf{P}^*(\mathbf{A}^*(\mathbf{A}\mathbf{v}_i) - \|\mathbf{A}\mathbf{v}_i\|^2 \cdot \mathbf{v}_i)).$$

- (b) **Compute minimum-energy direction in trial space.** Set

$$(1.2) \quad \mathbf{v}_{i+1} := \operatorname{argmin}\{\|\mathbf{A}\mathbf{z}\| : \mathbf{z} \in \operatorname{span}\{\mathbf{v}_{i-1}, \mathbf{v}_i, \mathbf{w}_i\}, \|\mathbf{z}\| = 1\}.$$

This minimization problem can be solved in $\mathcal{O}(mn)$ operations via an SVD of $\mathbf{A}[\mathbf{v}_{i-1}, \mathbf{v}_i, \mathbf{w}_i]$.

Under an appropriate condition on the singular value gap and the quality of the random embedding \mathbf{S} , we prove geometric convergence of \mathbf{v}_i to the right singular vector \mathbf{v}_{\min} of \mathbf{A} associated with the minimum singular value; empirically, we find it converges under much wider conditions than predicted by theory. For difficult problems with small singular value gaps or where one needs multiple singular vectors, one can use a block iterate $\mathbf{V}_i \in \mathbb{C}^{n \times b}$; see [subsection 2.3](#) for a discussion.

1.1. Illustrative example. To evaluate the RLOBPCG method, we consider a large-scale example that demonstrates its convergence behavior and efficiency relative to several established approaches. We compare the following methods:

1. RLOBPCG with the recommended implementation ([Algorithm 2.1](#)),
2. LOBPCG with the diagonal preconditioner $\mathbf{P} = \operatorname{diag}(\|\mathbf{A}(:, i)\|^{-1})$,
3. LOBPCG with no preconditioner,
4. The Lanczos algorithm [[19](#), sec. 10.1] applied to $\mathbf{A}^*\mathbf{A}$ (equivalently, Golub–Kahan bidiagonalization [[19](#), sec. 10.4]),
5. The sketch-and-solve approximate minimum singular vector \mathbf{v}_0 [[36](#)], and
6. MATLAB's `svd` routine.

To ensure that all methods are compared under similar conditions, we initialize all of the iterative methods using the sketch-and-solve initialization \mathbf{v}_0 . We test two examples, of dimension $m = 2 \cdot 10^6$ by $n = 4 \cdot 10^3$:

- **Easy.** To create an easy problem $\mathbf{A} = \mathbf{U} \operatorname{diag}(\sigma_1, \dots, \sigma_n) \mathbf{V}^*$, we generate \mathbf{V} using the MATLAB command

$$\mathbf{V} = \operatorname{orth}(\operatorname{diag}(\operatorname{randn}(n, 1)) + 1e-4 * \operatorname{randn}(n)) \in \mathbb{R}^{n \times n},$$

we let $\mathbf{U} \in \mathbb{R}^{m \times n}$ be a Haar-random matrix with orthonormal columns, and we set the first $n - 1$ singular values $\sigma_1, \dots, \sigma_{n-1}$ to be geometrically spaced between 1 and 0.1 and the smallest singular value to be $\sigma_n := 10^{-7}$. This problem is relatively easy because there is a large gap between the smallest and second-smallest singular values. Also, the right singular vectors are coherent (well-aligned with the standard basis vectors), making diagonal preconditioning fairly effective.

¹More traditionally, randomized preconditioning schemes typically use a QR decomposition of the sketch $\mathbf{S}\mathbf{A}$ rather than an SVD. We use an SVD here because it immediately yields the good initializations $\mathbf{v}_0 = \mathbf{v}_{-1}$. We will also use the singular value matrix Σ in our error estimates ([2.3](#)).

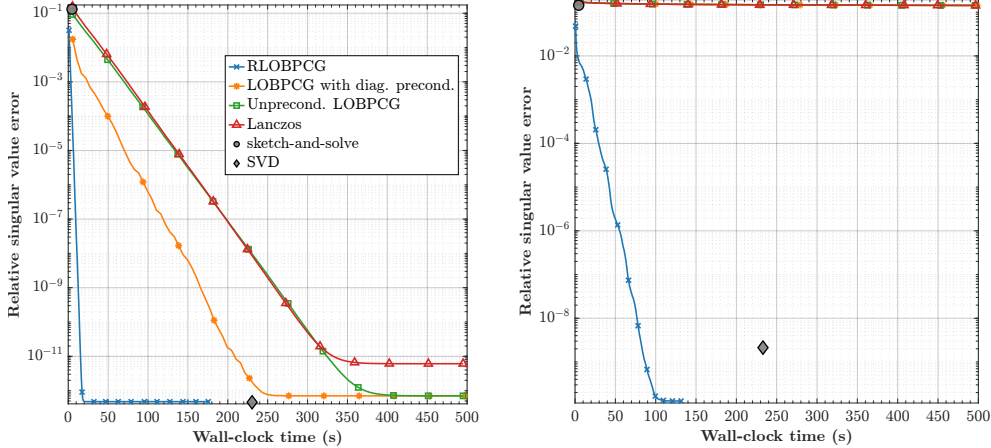


Fig. 1: Relative singular value error $(\|A\mathbf{v}_k\| - \sigma_n)/\sigma_n$ vs. wall-clock time for iterative minimum singular value algorithms on **easy** (left) and **hard** (right) problems.

- **Hard.** To generate a hard problem $\mathbf{A} = \mathbf{U} \text{diag}(\sigma_1, \dots, \sigma_n) \mathbf{V}^*$, we choose both $\mathbf{U} \in \mathbb{R}^{m \times n}$ and $\mathbf{V} \in \mathbb{R}^{n \times n}$ to be Haar-random, and we choose the singular values $\sigma_1, \dots, \sigma_n$ to be geometrically spaced between 1 and 10^{-10} . This problem is challenging because there is a small relative gap $(\sigma_{n-1}^2 - \sigma_n^2)/\sigma_n^2 \approx 0.05$ at the minimum singular value. It is also more difficult for the diagonally preconditioned LOBPCG method, because the problem is incoherent.

Figure 1 charts the relative error in the minimum singular value $(\|A\mathbf{v}_k\| - \sigma_n)/\sigma_n$ against wall-clock time for each method on both problems. On the **easy** problem (left), all of the iterative algorithms reach nearly the same accuracy as MATLAB's `svd` with differing convergence rates. Even on this easy problem, RLOBPCG is substantially faster than other methods, achieving maximal accuracy **12.1 × faster** than `svd`. On the **hard** problem (right), all of the non-RLOBPCG iterative methods fail to make any progress in the allotted time window. In contrast, RLOBPCG remains robust and rapidly convergent, attaining the same accuracy as the `svd` with a **2.8 × speedup**. This example highlights the effectiveness of randomized preconditioning, which preserves convergence even when other methods fail.

1.2. Summary of theoretical results. The experiments in the previous section suggest that the RLOBPCG method converges geometrically when there is a singular value gap. Our theoretical results confirm this to be the case.

To set the stage for our results, we employ the following standard definition:

DEFINITION 1.1 (Subspace embedding). *A (random) matrix $\mathbf{S} \in \mathbb{C}^{d \times m}$ is called a subspace embedding for a matrix $\mathbf{A} \in \mathbb{C}^{m \times n}$ with distortion $0 < \eta < 1$ if*

$$(1.3) \quad (1 - \eta) \|\mathbf{A}\mathbf{y}\|^2 \leq \|\mathbf{S}\mathbf{A}\mathbf{y}\|^2 \leq (1 + \eta) \|\mathbf{A}\mathbf{y}\|^2 \quad \text{for all } \mathbf{y} \in \mathbb{C}^n.$$

The concept of a subspace embedding is due to Sarlós [39]; see [22, sec. 5] for an introduction to idea. Most constructions of subspace embeddings are randomized and satisfy the condition (1.3) with high probability. Definitions of subspace embeddings in the literature differ on whether the norms in (1.3) are squared; we adopt the present

version as it is most convenient for our setting.

With this context, our main result for RLOBPCG is as follows:

THEOREM 1.2 (RLOBPCG: Convergence). *Let $\mathbf{A} \in \mathbb{C}^{m \times n}$ be a tall matrix with singular values $\sigma_1, \dots, \sigma_n > 0$, and let $\mathbf{S} \in \mathbb{C}^{d \times m}$ be a subspace embedding for \mathbf{A} with distortion $\eta \in [0, 1)$. Introduce the relative gap between the squared singular values*

$$\text{gap} := \frac{\sigma_{n-1}^2 - \sigma_n^2}{\sigma_n^2}.$$

Suppose that the distortion satisfies

$$(1.4) \quad \eta < \frac{\text{gap}}{2 + \text{gap}}.$$

Then \mathbf{v}_k , the approximation to \mathbf{v}_{\min} (the right singular vector of \mathbf{A} corresponding to the smallest singular value) after k iterations of RLOBPCG, satisfies

$$(1.5) \quad \frac{\|\mathbf{A}\mathbf{v}_k\|^2 - \sigma_n^2}{\sigma_n^2} \leq C \cdot \text{gap} \cdot q^{2k};$$

$$(1.6) \quad |\sin \angle(\mathbf{v}_k, \mathbf{v}_{\min})| \leq |\tan \angle(\mathbf{v}_k, \mathbf{v}_{\min})| \leq C^{1/2} \cdot q^k,$$

where the prefactor is $C = 2\eta/[(1 - \eta)\text{gap} - 2\eta]$ and the convergence rate is

$$(1.7) \quad q = \eta + \frac{1 - \eta}{1 + \text{gap}}.$$

As a corollary, we get a runtime guarantee for RLOBPCG.

COROLLARY 1.3 (RLOBPCG: Runtime). *Set $\eta := \min(\text{gap}/3, 1/6)$ and let $\varepsilon \in (0, 24]$. Execute RLOBPCG using a sparse sign embedding $\mathbf{S} \in \mathbb{C}^{d \times m}$ with embedding dimension $d = \mathcal{O}((n \log n)/\eta^2)$ and sparsity parameter $\mathcal{O}((\log n)/\eta)$. Then, with 99% probability, RLOBPCG produces a unit vector \mathbf{v}_k satisfying*

$$\|\mathbf{A}\mathbf{v}_k\|^2 \leq (1 + \varepsilon)\sigma_n^2$$

in $\mathcal{O}(\log(1/\varepsilon)/\min(\text{gap}, 1))$ iterations and

$$\mathcal{O}\left(\frac{\text{nnz}(\mathbf{A})}{\min(\text{gap}, 1)} \log\left(\frac{n}{\varepsilon}\right) + \frac{n^3 \log n}{\min(\text{gap}, 1)^2}\right) \text{ total operations.}$$

Here, $\text{nnz}(\mathbf{A})$ is the number of nonzero entries in \mathbf{A} .

We note several positive features of our result. First, LOBPCG is typically analyzed from an arbitrary starting vector \mathbf{v}_0 , which must satisfy strict requirements to ensure convergence to global minimum. The RLOBPCG method uses the “sketch-and-solve” starting vector \mathbf{v}_0 , which satisfies the appropriate conditions with high probability. Second, when implemented with an embedding of sufficiently small η relative to the singular value gap, RLOBPCG produces a high-quality preconditioner which ensures geometric convergence to the minimum singular value at a constant rate. In practice, we typically use an embedding with constant distortion η , which results in a convergence rate that depends on the gap. Our theoretical results require the stringent condition (1.4) ensuring the distortion of the embedding is small relative to the singular value gap. In practice, we have always observed convergence of $\|\mathbf{A}\mathbf{v}_k\|$ (perhaps

slowly) to the minimum singular value under the much weaker condition that η is a small constant bounded away from 1 (e.g., $\eta \leq 1/2$). Removing this limitation in our analysis seems challenging; proving global convergence from “generic” initialization or even characterizing the rate of convergence for preconditioned eigensolvers like LOBPCG remains an open problem [2, 4, 25, 35]. Our analysis of RLOBPCG uses results for preconditioned inverse iteration (PINVIT) [25] or preconditioned steepest descent [34], both of which are guaranteed to be outperformed by LOBPCG for a single step. More discussions and proofs appear in section 3.

1.3. Roadmap. The rest of the paper is structured as follows. Section 2 discusses implementation of RLOBPCG, choice of embedding, and a block version. Section 3 discusses theoretical results, and section 4 provides further experiments. We conclude in section 5 with an application to computing best rational approximations.

2. Algorithms and implementation. In this section, we discuss implementation details for RLOBPCG. In subsection 2.1, we describe the RLOBPCG algorithm and its implementation. Subsection 2.2 provides recommendations for the choice of the subspace embedding. Finally, in subsection 2.3, we discuss block implementations of RLOBPCG.

2.1. RLOBPCG implementation. Pseudocode for RLOBPCG is presented below in Algorithm 2.1, where MATLAB notation is used for matrix indexing. As outlined in the introduction, the RLOBPCG method consists of four main steps: (1) generate an embedding, (2) sketch and factorize, (3) define the preconditioner and initialization, and (4) apply LOBPCG to $\mathbf{A}^* \mathbf{A}$. Choice of embedding for step (1) is discussed in subsection 2.2, and steps (2) and (3) are straightforward: We compute the SVD of the sketch $\mathbf{S}\mathbf{A} = \tilde{\mathbf{U}}\tilde{\mathbf{S}}\tilde{\mathbf{V}}^T$ and set the preconditioner $\mathbf{P} = \tilde{\mathbf{V}}\tilde{\mathbf{S}}^{-1}$. The initial solution \mathbf{v}_0 is then set to be the smallest right singular vector of the sketch $\mathbf{S}\mathbf{A}$. For the rest of this section, we discuss step (4).

Orthogonalization and minimizing matrix–vector products. The dominant computational cost in LOBPCG consists of computing matrix–vector products with \mathbf{A} and orthogonalizing the basis for the energy-minimization step (1.2). Recall that each LOBPCG iteration computes the minimum-energy direction in a trial space

$$\mathbf{v}_{i+1} = \operatorname{argmin}\{\|\mathbf{A}\mathbf{z}\| : \mathbf{z} \in \operatorname{span}\{\mathbf{v}_{i-1}, \mathbf{v}_i, \mathbf{w}_i\}, \|\mathbf{z}\| = 1\}.$$

The search direction \mathbf{w}_i was defined above in (1.1). A direct implementation would orthogonalize the trial space $[\mathbf{v}_{i-1}, \mathbf{v}_i, \mathbf{w}_i]$ and perform Rayleigh–Ritz projection onto this basis at each iteration. This approach would require three matrix–vector products with \mathbf{A} and an orthogonalization of a three-dimensional basis per iteration. We can reduce this cost by carefully maintaining and updating the basis, reducing the cost to just one matrix–vector product per iteration [15, 21].

This efficient LOBPCG implementation for $\mathbf{A}^* \mathbf{A}$ is given in lines 5–24 of Algorithm 2.1. As the core “trick”, we introduce a vector \mathbf{x}_i (line 6) such that

$$(2.1) \quad \{\mathbf{v}_i, \mathbf{x}_i\} \text{ is an orthonormal basis for } \operatorname{span}\{\mathbf{v}_{i-1}, \mathbf{v}_i\}.$$

Since $\{\mathbf{v}_i, \mathbf{x}_i\}$ are orthonormal, only \mathbf{w}_i needs to be orthogonalized against these two vectors, and only a single matrix–vector product $\mathbf{A}\mathbf{w}_i$ is required per iteration (line 12). To combine speed and numerical stability, we perform orthogonalization by classical Gram–Schmidt with reorthogonalization (CGS2, 9–10). Faster but less stable approaches, such as SVQB [21, 41], are also possible for this step. It is important

Algorithm 2.1 RLOBPCG (single vector)

Input: Matrix $\mathbf{A} \in \mathbb{R}^{m \times n}$, tolerance $\tau \in [0, 1)$
Output: Minimum right singular vector $\mathbf{v} \in \mathbb{R}^n$ and singular value $\sigma \in \mathbb{R}_{\geq 0}$

```

1:  $\mathbf{S} \leftarrow 4n \times m$  SparseStack with sparsity  $\zeta = 4$ 
2:  $[\sim, \tilde{\Sigma}, \tilde{\mathbf{V}}] \leftarrow \text{SVD}(\mathbf{S}\mathbf{A})$  ▷ Sketch and take SVD
3:  $\mathbf{P} \leftarrow \tilde{\mathbf{V}}\tilde{\Sigma}^{-1}$  ▷ Build preconditioner
4:  $\mathbf{v}_0 \leftarrow \tilde{\mathbf{V}}(:, n)$ ,  $\mathbf{A}\mathbf{v}_0 \leftarrow \mathbf{A}\mathbf{v}_0$ ,  $\theta_0 \leftarrow \infty$  ▷ Sketch-and-solve initialization
5:  $\mathbf{r}_0 \leftarrow \mathbf{A}^*\mathbf{A}\mathbf{v}_0 - \|\mathbf{A}\mathbf{v}_0\|^2\mathbf{v}_0$  ▷ Initial residual
6:  $\mathbf{x}_0 \leftarrow []$ ,  $\mathbf{A}\mathbf{x}_0 \leftarrow []$  ▷ Initialize to empty; cf. (2.1)
7: for  $i = 0, 1, \dots, \text{max\_iter} - 1$  do ▷ Cap total iterations (e.g.,  $\text{max\_iter} = 200$ )
8:    $\mathbf{w}_i \leftarrow \mathbf{P}(\mathbf{P}^*\mathbf{r}_i)$  ▷ Compute search direction
9:    $\mathbf{w}_i \leftarrow \mathbf{w}_i - [\mathbf{v}_i, \mathbf{x}_i]([\mathbf{v}_i, \mathbf{x}_i]^*\mathbf{w}_i)$  ▷ Orthogonalize  $\mathbf{w}_i$  against  $[\mathbf{v}_i, \mathbf{x}_i]$ 
10:   $\mathbf{w}_i \leftarrow \text{NORMALIZE}(\mathbf{w}_i - [\mathbf{v}_i, \mathbf{x}_i]([\mathbf{v}_i, \mathbf{x}_i]^*\mathbf{w}_i))$  ▷ CGS2 for stability
11:   $\mathbf{T} \leftarrow [\mathbf{v}_i, \mathbf{x}_i, \mathbf{w}_i]$  ▷ Trial space
12:   $\mathbf{A}_T \leftarrow [\mathbf{A}\mathbf{v}_i, \mathbf{A}\mathbf{x}_i, \mathbf{A}\mathbf{w}_i]$  ▷ Matrix–vector product with trial space
13:   $[\sim, \Theta, \mathbf{C}] \leftarrow \text{SVD}(\mathbf{A}_T)$  ▷ Energy minimization (1.2)
14:   $\mathbf{v}_{i+1} \leftarrow \mathbf{T}\mathbf{C}(:, 3)$ ,  $\theta_{i+1} \leftarrow \Theta(3, 3)$  ▷ Updated next iterate
15:   $\mathbf{A}\mathbf{v}_{i+1} \leftarrow \mathbf{A}_T\mathbf{C}(:, 3)$  ▷ Updated  $\mathbf{A}\mathbf{v}_{i+1}$ 
16:   $\mathbf{r}_{i+1} \leftarrow \mathbf{A}^*\mathbf{A}\mathbf{v}_{i+1} - \theta_{i+1}^2\mathbf{v}_{i+1}$  ▷ Residual
17:  if  $\text{MOD}(i, 5) = 0$  then ▷ Check for convergence every five iterations
18:     $\text{tol\_check} \leftarrow (\|\mathbf{r}_{i+1}\| \leq \tilde{\Sigma}(1, 1)^2 \cdot \tau)$  ▷ Tolerance (2.3)
19:     $\text{stag\_check\_1} \leftarrow (1.1\|\mathbf{r}_{i+1}\| \geq \|\mathbf{r}_{i-4}\|)$ 
20:     $\text{stag\_check\_2} \leftarrow (1.1 \cdot (\theta_{i-4} - \theta_{i+1})/\theta_i \geq (\theta_{i-9} - \theta_{i-4})/\theta_{i-4})$ 
21:    if  $\text{tol\_check}$  and  $\text{stag\_check\_1}$  and  $\text{stag\_check\_2}$  break
22:  end if
23:   $\mathbf{q} \leftarrow \text{NORMALIZE}(\mathbf{C}(1, 1:2)^*)$ 
24:   $\mathbf{x}_{i+1} \leftarrow \mathbf{T}\mathbf{C}(:, 1:2)\mathbf{q}$ ,  $\mathbf{A}\mathbf{x}_{i+1} \leftarrow \mathbf{A}_T\mathbf{C}(:, 1:2)\mathbf{q}$  ▷ Update  $\mathbf{x}_{i+1}, \mathbf{A}\mathbf{x}_{i+1}$ ; cf. (2.1)
25: end for
26:  $\mathbf{v} \leftarrow \mathbf{v}_{i+1}$ ,  $\sigma \leftarrow \theta_{i+1}$  ▷ Collect outputs

```

to note that as \mathbf{v}_i converges to a singular vector, it becomes increasingly linearly dependent with \mathbf{v}_{i-1} . Therefore, the orthogonalization step is crucial—skipping it or using unstable orthogonalization methods may introduce spurious singular values [23]. The energy-minimization step (1.2) is performed by an SVD (line 13).

Stopping criteria. To stop RLOBPCG, we employ a variant of the following backward error-based convergence criterion from [15]:

$$(2.2) \quad \frac{\|\mathbf{r}_i\|}{(\|\mathbf{A}\|^2 + \|\mathbf{A}\mathbf{v}_i\|^2)} \leq \tau,$$

where $\mathbf{r}_i = \mathbf{A}^*\mathbf{A}\mathbf{v}_i - \|\mathbf{A}\mathbf{v}_i\|^2\mathbf{v}_i$ is the residual and $\tau \in [0, 1)$ is a tolerance parameter. To implement (2.2), we need to compute or estimate $\|\mathbf{A}\|$. By the subspace embedding property (Definition 1.1), the sketch $\mathbf{S}\mathbf{A}$ provides a good approximation to the singular values of \mathbf{A} , so that $\|\mathbf{A}\| \approx \|\mathbf{S}\mathbf{A}\| = \tilde{\Sigma}(1, 1)$ for $\tilde{\Sigma}$ computed in line 2 of Algorithm 2.1. Using this estimate with the bound $\|\mathbf{A}\mathbf{v}_i\| \leq \|\mathbf{A}\|$, we recommend the following convergence criterion:

$$(2.3) \quad \|\mathbf{r}_i\| \leq \tilde{\Sigma}(1, 1)^2 \cdot \tau.$$

A similar sketch-based estimate of $\|\mathbf{A}\|$ is also used in [15].

If one wants the maximum-achievable accuracy, we have not found the stopping rule (2.3) to be reliable on its own, and we were unable to find a way of setting the tolerance τ that reliably ensured the method both always halted and achieved near-optimal accuracy. Thus, we recommend using the stopping rule (2.3) with the conservative tolerance $\tau = 2n^{1/2}\varepsilon_{\text{mach}}$ and supplementing with two additional checks for stagnation, performed every five iterations:

$$(2.4) \quad 1.1\|\mathbf{r}_i\| \geq \|\mathbf{r}_{i-5}\| \quad \text{and} \quad 1.1 \cdot (\theta_{i-5} - \theta_i)/\theta_i \geq (\theta_{i-10} - \theta_{i-5})/\theta_{i-5}.$$

Here, θ_i is the approximation to the minimum singular produced at iteration i . The method is halted when both the tolerance (2.3) and the stagnation checks (2.4) are satisfied.

2.2. Choice of embedding. RLOBPCG can be implemented with any matrix $\mathbf{S} \in \mathbb{C}^{d \times m}$ satisfying the subspace embedding property (Definition 1.1); see [27, secs. 8–9] and [28, chs. 2, 6, & 7] for a survey of constructions. Based on the testing in [7, 13, 16], we recommend using SparseStack embeddings:

$$\mathbf{S} = \zeta^{-1/2} [\mathbf{s}_1 \quad \cdots \quad \mathbf{s}_m],$$

where each column \mathbf{s}_i is divided into ζ equally sized pieces, each of which has a single nonzero entry with uniformly random value ± 1 placed in uniformly random position. The parameter $1 \leq \zeta \leq d$ controls the level of sparsity.

How should one pick the parameters d and ζ ? Seminal analysis by Cohen [11] yields the following choices:

FACT 2.1 (SparseStack). *Fix a matrix $\mathbf{A} \in \mathbb{R}^{m \times n}$ and $\eta \in (0, 1)$. A SparseStack is a subspace embedding for \mathbf{A} for some $d = \mathcal{O}(n \log(n)/\eta^2)$ and sparsity $\zeta = \mathcal{O}(\log(n)/\eta)$ with distortion η with 99% probability.*

Analyses of different sparse dimensionality reduction maps with a different dependency of d and ζ on n and η appear in [7, 9, 10, 44]. In practice, we use parameters

$$2n \leq d \leq 4n \quad \text{and} \quad \zeta = 4,$$

which we find reliably yields an embedding of sufficient quality for our purposes.

2.3. Block version. If we are interested in obtaining a minimum right singular subspace rather than a single minimum right singular vector, we turn to block methods. Block methods are particularly useful when the minimum right singular vector is ill-conditioned because the gap between the smallest and second smallest singular values is very small. In such cases, projection-based methods struggle to isolate the target (minimum) singular vector [29, 30], and block methods targeting a singular subspace are more appropriate. Block methods are also more robust to singular value clustering [35, 49] and make use of hardware-efficient BLAS3 matrix operations.

A block version of RLOBPCG is presented in Algorithm 2.2. It is structurally similar to the single vector version (Algorithm 2.1), with the main change being the move from 1-dimensional to a b -dimensional subspace for a user-specified block size b . Instead of a vector initialization, we now provide an initial subspace using the sketch in line 4, which serves as a crude-but-effective approximation to the minimum b right singular vectors of \mathbf{A} [36]. In lines 7 and 18, the residual is now a matrix whose columns are the residual vectors for each of the b minimum singular vectors we wish to approximate. In lines 11–12, we apply *block* CGS2 (BCGS2) to orthogonalize

Algorithm 2.2 RLOBPCG (block version)

Input: Matrix $\mathbf{A} \in \mathbb{R}^{m \times n}$, block size b , tolerance $\tau \in [0, 1)$
Output: Minimum right singular subspace $\mathbf{V} \in \mathbb{R}^{n \times b}$ and diagonal matrix containing the minimum singular values $\mathbf{\Sigma} \in \mathbb{R}^{b \times b}$

```

1:  $\mathbf{S} \leftarrow 4n \times m$  SparseStack with sparsity  $\zeta = 4$ 
2:  $[\sim, \tilde{\mathbf{\Sigma}}, \tilde{\mathbf{V}}] \leftarrow \text{SVD}(\mathbf{S}\mathbf{A})$  ▷ Sketch and take SVD
3:  $\mathbf{P} \leftarrow \tilde{\mathbf{V}}\tilde{\mathbf{\Sigma}}^{-1}$  ▷ Build preconditioner
4:  $\mathbf{V}_0 \leftarrow \tilde{\mathbf{V}}(:, n-b+1:n)$ ,  $\mathbf{A}_{\mathbf{V}_0} \leftarrow \mathbf{A}\mathbf{V}_0$  ▷ Sketch-and-solve initialization
5:  $[\mathbf{C}, \mathbf{\Theta}] \leftarrow \text{RAYLEIGHRITZ}(\mathbf{A}_{\mathbf{V}_0}, \mathbf{V}_0)$ 
6:  $\mathbf{V}_0 \leftarrow \mathbf{V}_0\mathbf{C}$ ,  $\mathbf{A}_{\mathbf{V}_0} \leftarrow \mathbf{A}_{\mathbf{V}_0}\mathbf{C}$ 
7:  $\mathbf{R}_0 \leftarrow \mathbf{A}^*\mathbf{A}_{\mathbf{V}_0} - \mathbf{V}_0\mathbf{\Theta}^2$ 
8:  $\mathbf{X}_0 \leftarrow [], \mathbf{A}_{\mathbf{X}_0} \leftarrow []$  ▷ Initialize to empty
9: for  $i = 0, 1, \dots, \text{max\_iter} - 1$  do ▷ Cap total iterations (e.g.,  $\text{max\_iter} = 100$ )
10:    $\mathbf{W}_i \leftarrow \mathbf{P}(\mathbf{P}^*\mathbf{R}_i)$ 
11:    $\mathbf{W}_i \leftarrow \mathbf{W}_i - [\mathbf{V}_i, \mathbf{X}_i]([\mathbf{V}_i, \mathbf{X}_i]^*\mathbf{W}_i)$  ▷ Orthogonalize  $\mathbf{W}_i$  against  $[\mathbf{V}_i, \mathbf{X}_i]$ 
12:    $\mathbf{W}_i \leftarrow \text{ORTH}(\mathbf{W}_i - [\mathbf{V}_i, \mathbf{X}_i]([\mathbf{V}_i, \mathbf{X}_i]^*\mathbf{W}_i))$  ▷ BCGS2 for stability
13:    $\mathbf{T} \leftarrow [\mathbf{V}_i, \mathbf{X}_i, \mathbf{W}_i]$  ▷ Trial space
14:    $\mathbf{A}_{\mathbf{T}} \leftarrow [\mathbf{A}_{\mathbf{V}_i}, \mathbf{A}_{\mathbf{X}_i}, \mathbf{A}_{\mathbf{W}_i}]$  ▷ Matrix–vector products with trial space
15:    $[\sim, \mathbf{\Theta}, \mathbf{C}] \leftarrow \text{SVD}(\mathbf{A}_{\mathbf{T}})$  ▷ Rayleigh–Ritz
16:    $\mathbf{V}_{i+1} \leftarrow \mathbf{T}\mathbf{C}(:, 2b+1:3b)$  ▷ Updated next iterate
17:    $\mathbf{A}_{\mathbf{V}_{i+1}} \leftarrow \mathbf{A}_{\mathbf{T}}\mathbf{C}(:, 2b+1:3b)$  ▷ Updated  $\mathbf{A}\mathbf{V}_{i+1}$ 
18:    $\mathbf{R}_{i+1} \leftarrow \mathbf{A}^*\mathbf{A}_{\mathbf{V}_{i+1}} - \mathbf{V}_{i+1}\mathbf{\Theta}(2b+1:3b, 2b+1:3b)^2$  ▷ Residual matrix
19:   if  $\max_{1 \leq j \leq b} \|\mathbf{R}_{i+1}(:, j)\| \leq \tilde{\mathbf{\Sigma}}(1, 1)^2 \cdot \tau$  then break ▷ Better: also use (2.4)
20:    $\mathbf{Q} \leftarrow \text{ORTH}(\mathbf{C}(1:b, 1:2b)^*)$ 
21:    $\mathbf{X}_{i+1} \leftarrow \mathbf{T}\mathbf{C}(:, 1:2b)\mathbf{Q}$ ,  $\mathbf{A}_{\mathbf{X}_{i+1}} \leftarrow \mathbf{A}_{\mathbf{T}}\mathbf{C}(:, 1:2b)\mathbf{Q}$ 
22: end for
23:  $\mathbf{V} \leftarrow \mathbf{V}_{i+1}$ 
24:  $\mathbf{\Sigma} \leftarrow \mathbf{\Theta}(2b+1:3b, 2b+1:3b)$ 

```

the matrix search direction \mathbf{W}_i against both \mathbf{V}_i and \mathbf{X}_i . We stop the algorithm using a suitable modification of the stopping rule (2.3). For the best reliability, one can also use the stagnation checks (2.4). A more efficient block version would deflate the converged singular vectors, a process known as locking [23, 24]. Once an index j meets the condition (2.3), it would be locked by storing it in \mathbf{V}_i , but removing the corresponding columns from \mathbf{X}_i and \mathbf{W}_i . This ensures the trial space is orthogonal to converged singular vectors. Since we target only a small number of minimum singular vectors in this work, we omit this step. For details on locking, see [24, sec. 2.3].

3. Theory. In this section, we present convergence analysis of RLOBPCG. Subsections 3.1 and 3.2 provide background on the analysis of sketching and LOBPCG, subsection 3.3 discusses how to relate quantities in the LOBPCG convergence theory to the accuracy of singular values and singular vectors, and subsections 3.4 and 3.5 prove Theorem 1.2 and Corollary 1.3.

3.1. Background: Results for sketching. The definition of subspace embeddings appeared above in Definition 1.1. This section will review two necessary results about sketching: the quality of the randomized preconditioner \mathbf{P} and the quality of the “sketch-and-solve” initialization \mathbf{v}_0 . For the former, we employ the following result of Rokhlin & Tygert [38]; see [22, Prop. 5.4] for a modern proof.

FACT 3.1 (Randomized preconditioning). *Let $\mathbf{A} \in \mathbb{C}^{m \times n}$ be a full-rank matrix, and let $\mathbf{S} \in \mathbb{C}^{d \times m}$ be a subspace embedding for \mathbf{A} of distortion $\eta \in [0, 1)$. Introduce the preconditioner $\mathbf{P} = \mathbf{V}\Sigma^{-1}$ from an SVD $\mathbf{S}\mathbf{A} = \mathbf{U}\Sigma\mathbf{V}^*$. Then*

$$\frac{1}{1 + \eta} \leq \sigma_{\min}(\mathbf{A}\mathbf{P})^2 \leq \sigma_{\max}(\mathbf{A}\mathbf{P})^2 \leq \frac{1}{1 - \eta}.$$

To quantify the quality of the “sketch-and-solve” initialization $\mathbf{v}_0 = \mathbf{P}\mathbf{e}_n$ for RLOBPCG, we use the following result:

FACT 3.2 (Sketch-and-solve for minimum singular value). *Import the setting of Fact 3.1 and define $\mathbf{v}_0 := \mathbf{P}\mathbf{e}_n$. Then*

$$\|\mathbf{A}\mathbf{v}_0\|^2 \leq \frac{1 + \eta}{1 - \eta} \cdot \sigma_{\min}(\mathbf{A})^2.$$

Versions of this result appear in [36, Rem. 2.1], [22, Prop. 5.5]; see also [17].

3.2. Background: Preconditioned eigensolvers. Despite decades of interest, a sharp convergence theory for LOBPCG remains elusive. Therefore, to understand LOBPCG, it is common to compare the iterates of LOBPCG to other preconditioned eigensolvers, such as preconditioned inverse iteration (PINVIT, [33]) or preconditioned steepest descent [34], that are easier to analyze. We shall make use of this standard strategy to analyze RLOBPCG.

Given the current iterate $\mathbf{v} = \mathbf{v}_i$ and the previous iterate $\mathbf{v}_{\text{old}} = \mathbf{v}_{i-1}$, recall that the next iterate generated by LOBPCG is given by the equations

$$(3.1) \quad \mathbf{w} := \mathbf{P}(\mathbf{P}^*(\mathbf{A}^*(\mathbf{A}\mathbf{v}) - \|\mathbf{A}\mathbf{v}\|^2 \cdot \mathbf{v})),$$

$$(3.2) \quad \mathbf{v}_{\text{LOBPCG}} := \operatorname{argmin}\{\|\mathbf{A}\mathbf{z}\| : \mathbf{z} \in \operatorname{span}\{\mathbf{v}_{\text{old}}, \mathbf{v}, \mathbf{w}\}, \|\mathbf{z}\| = 1\}.$$

The next iterate $\mathbf{v}_{\text{LOBPCG}}$ generated by LOBPCG depends on both the previous iterates \mathbf{v} and \mathbf{v}_{old} and the search direction \mathbf{w} . The preconditioned steepest descent iteration is the same as LOBPCG, except the dependence on the past state \mathbf{v}_{old} is removed:

$$(3.3) \quad \mathbf{v}_{\text{PSD}} := \operatorname{argmin}\{\|\mathbf{A}\mathbf{z}\| : \mathbf{z} \in \operatorname{span}\{\mathbf{v}, \mathbf{w}\}, \|\mathbf{z}\| = 1\}.$$

Since LOBPCG searches over a larger set of possible vectors, the norm $\|\mathbf{A}\mathbf{v}\|$ is always smaller for LOBPCG than for preconditioned steepest descent:

$$(3.4) \quad \|\mathbf{A}\mathbf{v}_{\text{LOBPCG}}\| \leq \|\mathbf{A}\mathbf{v}_{\text{PSD}}\|.$$

The relation (3.4) allows us to transfer single-step bounds for preconditioned steepest descent to single-step bounds for LOBPCG.

We import the following standard bound for PINVIT with an optimal damping factor [34, Thm. 1.1] and specialize to our setting.

FACT 3.3 (Preconditioned steepest descent). *Let $\mathbf{v} \in \mathbb{C}^n$ be a vector, let $\mathbf{A} \in \mathbb{C}^{m \times n}$ be a full-rank matrix with singular values $\sigma_1, \dots, \sigma_n$, and let $\mathbf{P} \in \mathbb{C}^{n \times n}$ be a full-rank preconditioner. Introduce the parameter*

$$(3.5) \quad \gamma := \inf_{t > 0} \|\mathbf{I} - t\mathbf{P}^*\mathbf{A}^*\mathbf{A}\mathbf{P}\|.$$

Assume that the unit vector \mathbf{v} satisfies $\sigma_i \leq \|\mathbf{A}\mathbf{v}\| < \sigma_{i-1}$ and introduce the gap

$$\operatorname{gap}_i := \frac{\sigma_{i-1}^2 - \sigma_i^2}{\sigma_i^2}.$$

Then the preconditioned steepest descent iterate (3.3) either is below the i th singular value $\|\mathbf{A}\mathbf{v}_{\text{PSD}}\| \leq \sigma_i$ or it admits the bound

$$\frac{\|\mathbf{A}\mathbf{v}_{\text{PSD}}\|^2 - \sigma_i^2}{\sigma_{i-1}^2 - \|\mathbf{A}\mathbf{v}_{\text{PSD}}\|^2} \leq q^2 \cdot \frac{\|\mathbf{A}\mathbf{v}\|^2 - \sigma_i^2}{\sigma_{i-1}^2 - \|\mathbf{A}\mathbf{v}\|^2} \quad \text{for } q = \gamma + \frac{1-\gamma}{1+\text{gap}_i}.$$

Applying the comparison (3.4), specializing to the minimum singular value (i.e., $i = n$), and iterating, we obtain a bound for LOBPCG:

$$(3.6) \quad \frac{\|\mathbf{A}\mathbf{v}_k\|^2 - \sigma_n^2}{\sigma_{n-1}^2 - \|\mathbf{A}\mathbf{v}_k\|^2} \leq q^{2k} \cdot \frac{\|\mathbf{A}\mathbf{v}_0\|^2 - \sigma_n^2}{\sigma_{n-1}^2 - \|\mathbf{A}\mathbf{v}_0\|^2} \quad \text{provided } \|\mathbf{A}\mathbf{v}_0\| < \sigma_{n-1}.$$

3.3. Interpreting (3.6). The bound (3.6) may not initially seem very transparent. Before proving our main theorem, let us simplify. First, we bound the approximate minimum singular value $\|\mathbf{A}\mathbf{v}\|$, then we treat the angle $\angle(\mathbf{v}, \mathbf{v}_{\min})$ with the minimum singular vector. These results are more-or-less standard, and we review them for completeness.

We begin with the approximate minimum singular value $\|\mathbf{A}\mathbf{v}\|$. Introduce the parameter

$$\text{gap} := \text{gap}_n = \frac{\sigma_{n-1}^2 - \sigma_n^2}{\sigma_n^2}.$$

as in Theorem 1.2, and write B for the right-hand side of (3.6). Using these notations, (3.6) can be written

$$\|\mathbf{A}\mathbf{v}_k\|^2 - \sigma_n^2 \leq B \cdot ((1 + \text{gap})\sigma_n^2 - \|\mathbf{A}\mathbf{v}_k\|^2).$$

Rearranging gives

$$\frac{\|\mathbf{A}\mathbf{v}_k\|^2 - \sigma_n^2}{\sigma_n^2} \leq \frac{B}{1+B} \cdot \text{gap} \leq B \cdot \text{gap}.$$

Reinstating the definition of B as the right-hand side of (3.6), we obtain

$$(3.7) \quad \frac{\|\mathbf{A}\mathbf{v}_k\|^2 - \sigma_n^2}{\sigma_n^2} \leq q^{2k} \cdot \frac{\|\mathbf{A}\mathbf{v}_0\|^2 - \sigma_n^2}{\sigma_{n-1}^2 - \|\mathbf{A}\mathbf{v}_0\|^2} \cdot \text{gap} \quad \text{provided } \|\mathbf{A}\mathbf{v}_0\| < \sigma_{n-1}.$$

The bound (3.7) may be easier to interpret than the original expression (3.6).

Now we examine the angle $\angle(\mathbf{v}, \mathbf{v}_{\min})$. Any unit vector \mathbf{v} we may write as a linear combination

$$\mathbf{v} = \alpha \mathbf{v}_{\min} + \beta \mathbf{v}_{\perp} \quad \text{with } |\alpha|^2 + |\beta|^2 = 1$$

of \mathbf{v}_{\min} and a unit vector \mathbf{v}_{\perp} orthogonal to \mathbf{v}_{\min} . The sine of the angle between \mathbf{v} and \mathbf{v}_{\min} is $|\sin \angle(\mathbf{v}, \mathbf{v}_{\min})| = |\beta|$. We have the decomposition

$$\|\mathbf{A}\mathbf{v}\|^2 = |\alpha|^2 \sigma_n^2 + |\beta|^2 \|\mathbf{A}\mathbf{v}_{\perp}\|^2 = (1 - \sin^2 \angle(\mathbf{v}, \mathbf{v}_{\min}))\sigma_n^2 + \sin^2 \angle(\mathbf{v}, \mathbf{v}_{\min}) \|\mathbf{A}\mathbf{v}_{\perp}\|^2.$$

Since \mathbf{v}_{\perp} is orthogonal to \mathbf{v}_{\min} , $\|\mathbf{A}\mathbf{v}_{\perp}\|^2 \geq \sigma_{n-1}^2$. Thus,

$$\|\mathbf{A}\mathbf{v}\|^2 \geq (1 - \sin^2 \angle(\mathbf{v}, \mathbf{v}_{\min}))\sigma_n^2 + \sin^2 \angle(\mathbf{v}, \mathbf{v}_{\min})\sigma_{n-1}^2.$$

Rearranging yields

$$\sin^2 \angle(\mathbf{v}, \mathbf{v}_{\min}) \leq \frac{\|\mathbf{A}\mathbf{v}\|^2 - \sigma_n^2}{\sigma_{n-1}^2 - \sigma_n^2}.$$

Thus

$$\tan^2 \angle(\mathbf{v}, \mathbf{v}_{\min}) = \frac{\sin^2 \angle(\mathbf{v}, \mathbf{v}_{\min})}{1 - \sin^2 \angle(\mathbf{v}, \mathbf{v}_{\min})} \leq \frac{\frac{\|\mathbf{A}\mathbf{v}\|^2 - \sigma_n^2}{\sigma_{n-1}^2 - \sigma_n^2}}{1 - \frac{\|\mathbf{A}\mathbf{v}\|^2 - \sigma_n^2}{\sigma_{n-1}^2 - \sigma_n^2}} = \frac{\|\mathbf{A}\mathbf{v}\|^2 - \sigma_n^2}{\sigma_{n-1}^2 - \|\mathbf{A}\mathbf{v}\|^2}.$$

Combining this bound with (3.6) yields

$$(3.8) \quad |\tan \angle(\mathbf{v}, \mathbf{v}_{\min})| \leq q^k \cdot \left(\frac{\|\mathbf{A}\mathbf{v}_0\|^2 - \sigma_n^2}{\sigma_{n-1}^2 - \|\mathbf{A}\mathbf{v}_0\|^2} \right)^{1/2} \quad \text{provided } \|\mathbf{A}\mathbf{v}_0\| < \sigma_{n-1}.$$

3.4. Proof of Theorem 1.2. In order to instantiate the bound (3.6), we must bound the parameter γ in (3.5) and ensure that $\|\mathbf{A}\mathbf{v}_0\| < \sigma_{n-1}$.

First, we bound γ . By Fact 3.1, the squared singular values of $\mathbf{A}\mathbf{P}$ lie between $1/(1+\eta)$ and $1/(1-\eta)$. Ergo,

$$\gamma = \inf_{t>0} \|\mathbf{I} - t\mathbf{P}^* \mathbf{A}^* \mathbf{A}\mathbf{P}\| \leq \inf_{t>0} \max \left\{ \frac{t}{1-\eta} - 1, 1 - \frac{t}{1+\eta} \right\}.$$

The right-hand side is minimized by taking $t = 1 - \eta^2$, yielding the bound $\gamma \leq \eta$.

Next, we establish $\|\mathbf{A}\mathbf{v}_0\| < \sigma_{n-1}$. By Fact 3.2, the \mathbf{v}_0 satisfies

$$(3.9) \quad \|\mathbf{A}\mathbf{v}_0\|^2 \leq \frac{1+\eta}{1-\eta} \cdot \sigma_n^2.$$

The right-hand side is strictly less than σ_{n-1}^2 under the hypothesis (1.4).

Finally, we bound the quantity

$$\frac{\|\mathbf{A}\mathbf{v}_0\|^2 - \sigma_n^2}{\sigma_{n-1}^2 - \|\mathbf{A}\mathbf{v}_0\|^2}$$

Using the bound (3.9) and the definition $\sigma_{n-1}^2 = (1 + \text{gap})\sigma_n^2$, we have

$$\frac{\|\mathbf{A}\mathbf{v}_0\|^2 - \sigma_n^2}{\sigma_{n-1}^2 - \|\mathbf{A}\mathbf{v}_0\|^2} \leq \frac{\frac{1+\eta}{1-\eta} - 1}{1 + \text{gap} - \frac{1+\eta}{1-\eta}} = \frac{2\eta}{(1-\eta)\text{gap} - 2\eta}.$$

The conclusions (1.5) and (1.6) of the theorem follow from this equation and the bounds (3.7) and (3.8) from the previous section.

3.5. Proof of Corollary 1.3. Since $\eta = \min(\text{gap}/3, 1/6)$, the convergence rate q from (1.7) satisfies the bound $q \leq 1 - \min(\text{gap}, 1)/6$. Further, we have the bound $C \cdot \text{gap} \leq 2$. The claimed complexity results follow from Theorem 1.2 and Fact 2.1.

4. Experiments. This section presents a set of numerical experiments designed to evaluate the accuracy, robustness, and efficiency of RLOBPCG (Algorithm 2.1) for computing the smallest singular value and its associated singular vector. All

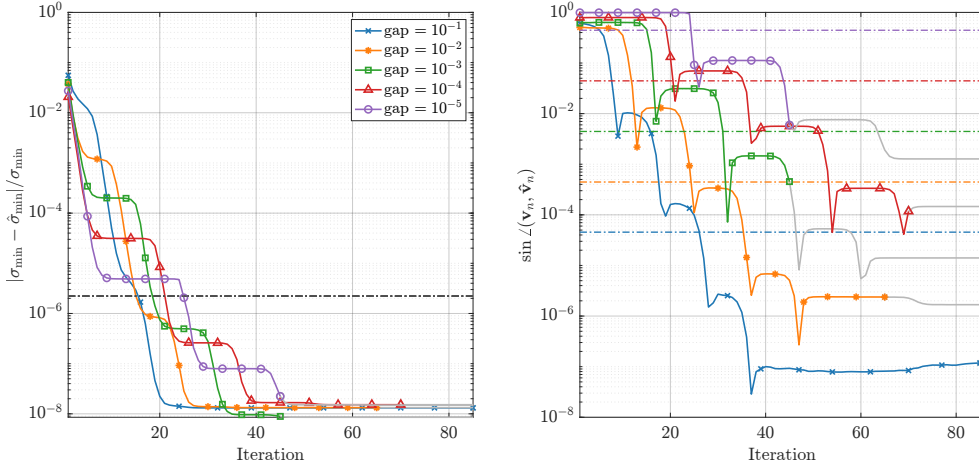


Fig. 2: Convergence behavior of singular values (left) and singular vectors (right) of RLOBPCG on matrices with different singular value gaps. Dashed lines show predictions from matrix perturbation theory.

experiments were performed in MATLAB version 2024b on a workstation with Intel Xeon Gold 6538Y+ CPU @ 2.40GHz (128 cores) and 2TB memory.

Each curve will be divided into an *active* and a *inactive* segment. The active portion (colored) corresponds to iterations before which RLOBPCG the convergence criteria (2.3) and (2.4) have not been met. Once these criteria have been met, the curve transitions to the gray inactive part. For a given approximation $\hat{\mathbf{v}}_{\min}$ to the minimum singular vector and its corresponding singular value approximation $\hat{\sigma}_{\min}$, we will plot both the singular value error $|\hat{\sigma}_{\min} - \sigma_{\min}|/\sigma_{\min}$ and the angle $\sin \angle(\mathbf{v}_{\min}, \hat{\mathbf{v}}_{\min})$ to the true minimum singular vector. In all plots, dashed horizontal lines indicate the level of accuracy predicted by matrix perturbation theory [12, 47] for a backward stable algorithm. For the relative singular value $|\hat{\sigma}_{\min} - \sigma_{\min}|/\sigma_{\min}$, the expected error is $u \cdot \sigma_{\max}/\sigma_{\min}$ and for the angle $\sin \angle(\mathbf{v}_{\min}, \hat{\mathbf{v}}_{\min})$, the expected error is $u/\text{gap}_{\text{abs}}$. Here, $u \approx 10^{-16}$ is the unit roundoff in double precision and $\text{gap}_{\text{abs}} = (\sigma_{n-1} - \sigma_n)/\sigma_1$ is the singular value gap.

4.1. Single-vector tests. In this section, we examine how the spectral gap and the condition number affect the performance of RLOBPCG. Throughout this subsection, \mathbf{A} is a $10^4 \times 10^2$ matrix with left and right singular vectors drawn from the Haar distribution.

4.1.1. Effect of the singular value gap. First, we investigate how the size of the (relative) singular value gap affects the convergence behavior of RLOBPCG. The singular values decay geometrically from 1 to 10^{-9} for the first $n - 2$ values. We set the smallest singular value to $\sigma_n = 10^{-10}$, and choose the second-smallest singular value σ_{n-1} to achieve a prescribed value of the gap, defined in section 3 as

$$\text{gap} = \frac{\sigma_{n-1}^2 - \sigma_n^2}{\sigma_n^2}.$$

Figure 2 display the convergence histories for both the minimum singular value

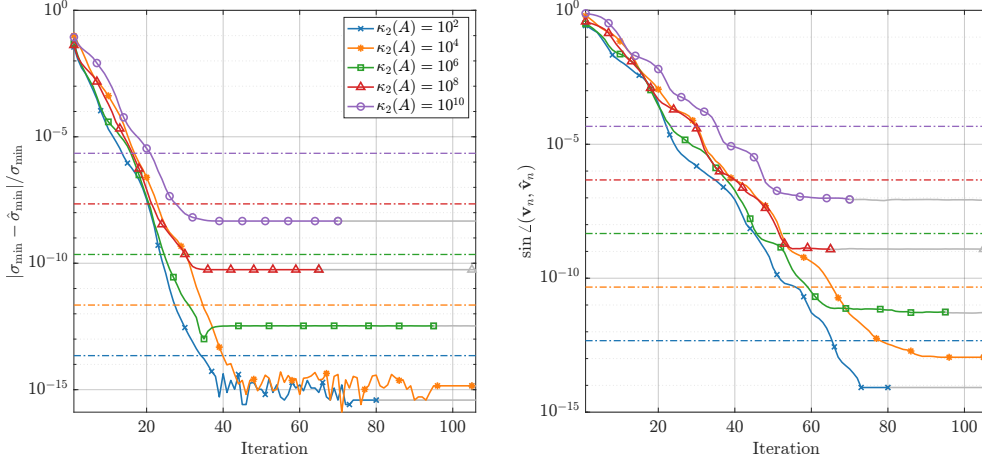


Fig. 3: Convergence behavior of singular values (*left*) and singular vectors (*right*) of RLOBPCG on matrices with different condition numbers. Dashed lines show predictions from matrix perturbation theory.

(*left*) and its associated singular vector (*right*). As the relative spectral gap becomes smaller, the problem becomes increasingly ill-conditioned (difficult), and the speed of convergence is affected. Nevertheless, RLOBPCG consistently achieves accuracy levels far better than the dashed lines predicted by perturbation theory for a stable algorithm.

When the gap is small, the singular vector error exhibits a “spiky” convergence profile where the error repeatedly drops rapidly, rises to a plateau, then drops again, before settling down at a final level of accuracy. This behavior is characteristic of nearly degenerate singular subspaces and has been observed in earlier empirical studies of iterative methods [48].

4.1.2. Effect of the condition number. Next, we explore how the condition number of the matrix affects the convergence of RLOBPCG. In this plot, the singular values decay geometrically from 10^{-8} to 10^{-10} for the smallest $n-1$ singular values, while the largest singular value is adjusted to yield a prescribed value for the condition number $\kappa_2(\mathbf{A}) = \sigma_1(\mathbf{A})/\sigma_n(\mathbf{A})$. The relative spectral gap remains constant across all test cases so that only the condition number varies between the curves.

Figure 3 shows the results. As the condition number increases, the maximum attainable accuracy of both quantities deteriorate due to the ill-conditioning of the problem, which amplifies roundoff errors. For the singular values, the limiting accuracy worsens proportionally to the condition number (this is largely due to the division by σ_n^2 for the relative error; the absolute error of the computed singular values is bounded by $O(u\|\mathbf{A}\|)$ throughout). For the singular vectors, the attained accuracy also worsens with the condition number, though RLOBPCG continues to achieve accuracy levels well below the accuracy level $u/\text{gap}_{\text{abs}}$ predicted by perturbation theory.

4.2. Block tests. We next investigate the block implementation of RLOBPCG detailed in subsection 2.3. The block method enables RLOBPCG to compute ap-

proximations to multiple singular value/vector triplets at once, and it can improve the reliability and rate of convergence of RLOBPCG *even when only one singular value/vector triplet is required*. Throughout this section, we will focus on this second use case and evaluate the accuracy of the minimum singular value and vectors computed by block RLOBPCG.

Experimental setup. In this experiment, we vary the block size $b \in \{1, 3, 5, 10, 20\}$ to assess how increasing the block dimension influences convergence and computational efficiency. We generate a test matrix of size $10^6 \times 2 \cdot 10^3$, with left and right singular vectors drawn from the Haar distribution and *clustered* singular values

$$\sigma_i(\mathbf{A}) = \exp\left(-\log(10^{10}) \cdot \left[\frac{i-1}{n-1}\right]^a\right), \quad i = 1, 2, \dots, n,$$

with $a = 1/256$. This problem has a small singular value gap $(\sigma_{n-1}^2 - \sigma_n^2)/\sigma_n^2 \approx 1.8 \times 10^{-3}$, making it a challenging problem for any iterative algorithm.

Measuring cost. There are several ways of measuring the cost of block LOBPCG. The simplest method is to count the number of *iterations* as a proxy for the cost of the algorithm. However, this metric is overly flattering to block methods, as the amount of work performed in each step of the algorithm increases with the block size. Thus, another natural metric would be the *number of matrix–vector products* with the matrix \mathbf{A} expended by each algorithm. Each step of the block method performs a matrix product \mathbf{AV} , which may be realized as b matrix–vector products. But the matrix–vector product count has its own issues, as it ignores the fact that modern computer processors perform matrix–matrix multiplication much faster than iterated matrix–vector multiplication. Therefore, in addition to these implementation and hardware-insensitive cost metrics, it is appropriate to also report the *wall-clock time* expended by each method. Given the merits and demerits of measuring cost with each of these metrics, we report all three in this section.

Results. Figure 4 presents the results. We highlight a few conclusions:

- **Which block size is fastest?** As discussed above, the relative performance of RLOBPCG with different block sizes is sensitive to the cost metric. In terms of iterations, the largest block size is most performant, and block size $b = 1$ minimizes the number of matrix–vector products. In terms of wall-clock time, the speed of convergence is essentially indistinguishable for block sizes $b \leq 5$. In particular, on this example, block size $b = 1$ is essentially optimal for both matrix–vector cost and wall-clock time. This behavior is different than randomized block Krylov algorithms for low-rank approximation and computation of dominant singular values and vectors, which generally show wall-clock time speedups with a (modestly) large block size [8, 37, 45].
- **Stopping criteria.** As these examples highlight, stopping RLOBPCG in the presence of both ill-conditioning and small singular value gaps is challenging. In all cases, we continue to observe convergence after the method is stopped using our criteria. However, using a large block size is seen to forestall early termination, because our stopping criteria requires all singular values in the block to converge before terminating.
- **Attained accuracy.** For the singular values, the maximum attained accuracy for RLOBPCG is relatively insensitive to the block size. However, for the accuracy of the *singular vector*, using a larger block size of $b \geq 5$ is seen to improve the accuracy by 1.5 orders of magnitude.

These findings are nuanced and defy a simple description of the effect of the block size

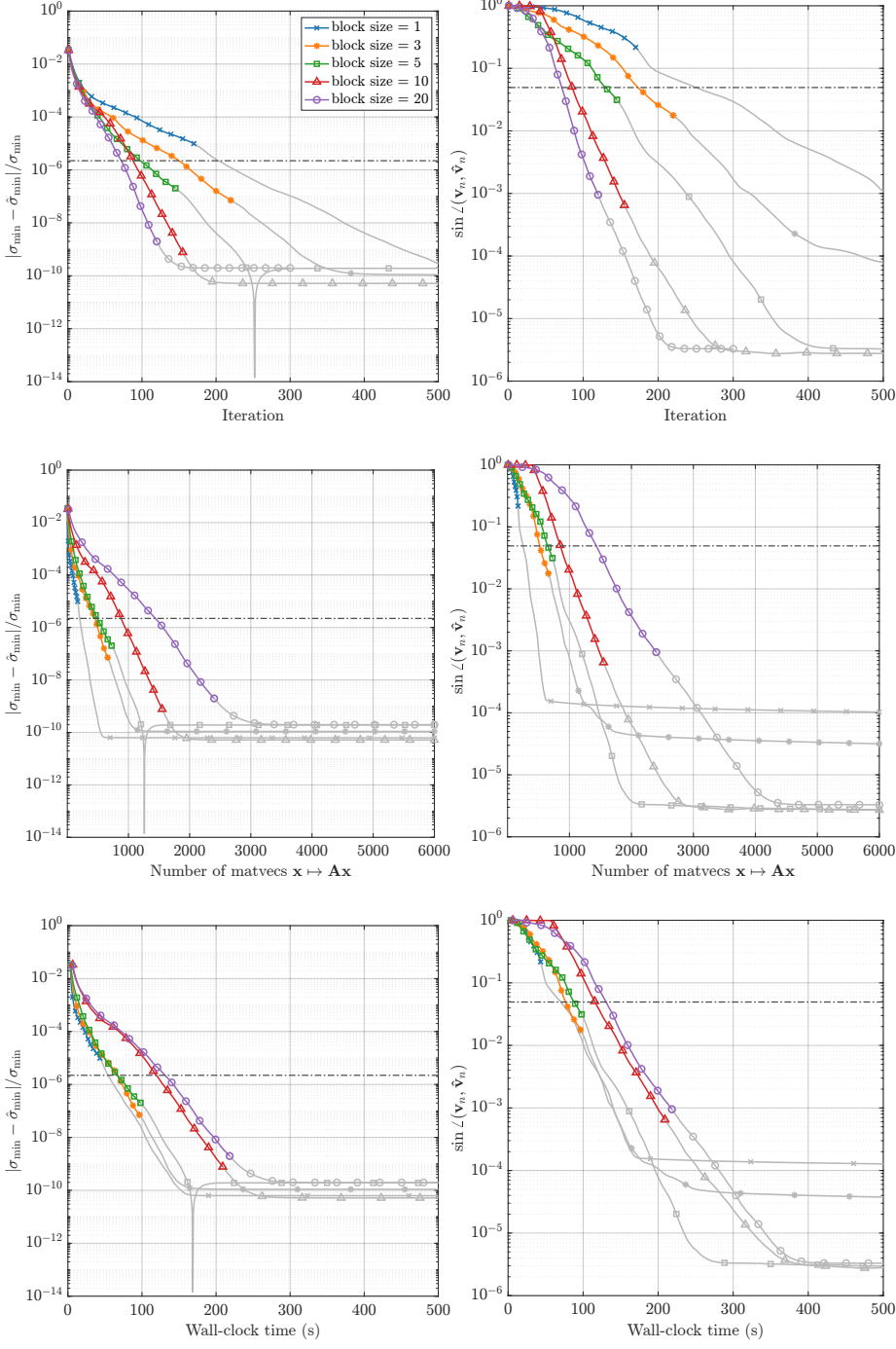


Fig. 4: Singular value (left) and singular vector (right) error as a function of iteration count (top), total number of matrix-vector products (middle), and wall-clock time (bottom) for RLOBPCG with various block sizes. Dashed lines show predictions from matrix perturbation theory.

on the performance of the method. Still, we believe these experiments do demonstrate that, for problems such as this with small singular value gaps, the RLOBPCG method with small block size $b \in \{3, 5\}$ can have benefits in accuracy and reliability over the unblocked version with minimal impact on the computational cost.

5. Application: Rational approximation. The AAA-Lawson algorithm [32] attempts to compute the best (minimax) rational approximation r_* to a function $f : \Omega \rightarrow \mathbb{C}$ in the sense that

$$\|r - f\|_\infty := \max_{z \in \Omega} |r(z) - f(z)|$$

is minimized in a domain $\Omega \subseteq \mathbb{C}$ over all type- $(n-1, n-1)$ rational functions (i.e., those that may be expressed as the ratio of two degree- $(n-1)$ polynomials). Under mild conditions (smoothness of f and Ω), the minimax approximant r_* is that the error $f - r_*$ exhibits a near-circular curve [42] with winding number generically equal to $2n+1$; the corresponding effect for real functions is the perfectly equioscillating error curve [43, ch. 24].

Computationally, the AAA-Lawson algorithm proceeds as follows. First compute use the AAA algorithm [31] to compute an initial approximant of type $(n-1, n-1)$. Then refine the approximation r by solving a sequence of the minimum singular vector problem for a matrix of the form $W\mathbf{A} \in \mathbb{C}^{m \times n}$, wherein $W \in \mathbb{C}^{m \times m}$ is a diagonal “weight” matrix that gets updated at each step. This results in an iteratively reweighted nullspace problem; here we employ RLOBPCG for each of these.

AAA-Lawson provides a natural setting to test RLOBPCG, as the matrix \mathbf{A} needs to be very tall-skinny to accurately represent the near-circularity of the error curve, and hence to obtain the minimax solution of high accuracy; this is unlike the standard AAA algorithm, for which it is often possible to work with matrices of constant aspect ratio $m = O(n)$, e.g., using an adaptive sampling strategy [14].

To evaluate the proposed combination of AAA-Lawson and RLOBPCG, we consider approximating the function

$$f(z) = z \operatorname{sign}(\operatorname{Re}(z)),$$

with Ω chosen to be the union of unit circles centered at 1.03 and -1.03 . This problem is challenging because the function f has a singularity along the line $\operatorname{Re}(z) = 0$, which the region Ω is close to.

We use 10,000 uniformly distributed points on each circle, resulting in $m = 20,000$ points in total, and find a degree 100 rational approximation. The main cost lies in computing the SVD of a $20,000 \times 101$ matrix. We compare four algorithms: (i) standard AAA (which does not aim to be minimax), (ii) AAA-Lawson, (iii) AAA-Lawson where we use sketch-and-solve for the tall-skinny SVDs (which is not expected to yield a minimax approximation), (iv) AAA-Lawson where RLOBPCG is used. For (ii), (iii), and (iv), we performed 100 Lawson steps.

The resulting execution time and error curves are shown in section 5. Observe that the methods based on AAA-Lawson are able to reduce the error by about an order of magnitude as compared with AAA (which is a typical behavior), while the use of RLOBPCG results in more than twice faster runtime compared with standard AAA-Lawson (which uses MATLAB’s `svd`). Note that here we used only the stopping criterion (2.3) with $\tau = 10^{-15}$; when we also used the stagnation checks (2.4), AAA-Lawson with RLOBPCG further improved the error curve to near-circular (and thus

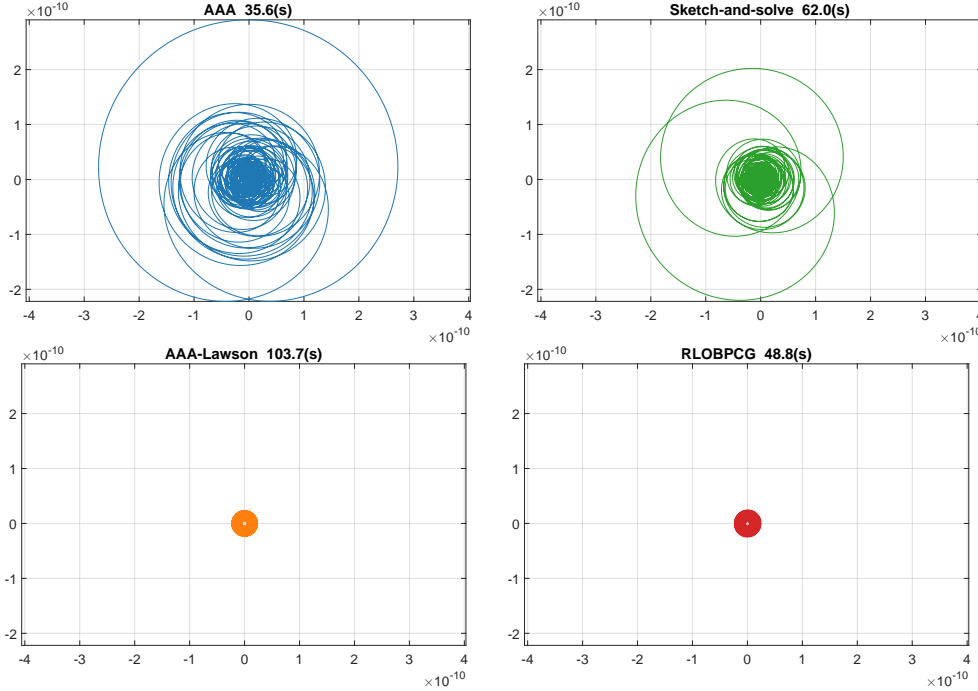


Fig. 5: Error curve $r - f$ of rational approximation to $f(z) = z \operatorname{sign}(\operatorname{Re}(z))$ for AAA (top left) and AAA-Lawson with MATLAB's `svd` (bottom left), sketch-and-solve (top right), and RLOBPCG (bottom right).

reducing $\|f - r\|_\infty$ by a factor ≈ 2.5), while the execution time increased to roughly the same as standard AAA-Lawson.

6. Conclusion. This work introduces RLOBPCG, a randomized method for computing a small number of the smallest singular values and associated right singular vectors of very tall matrices. The algorithm combines randomized preconditioning with the LOBPCG eigensolver applied to the normal equations. We prove geometric convergence under the standard subspace embedding assumption and a spectral gap condition. Numerical experiments demonstrate that randomized preconditioning significantly improves robustness and efficiency over classical iterative approaches, achieving high accuracy even in ill-conditioned and small-gap regimes. A block variant further improves the method's flexibility.

Several questions remain open. First, the current convergence theory requires a dependence between embedding distortion and the spectral gap; extending the analysis to weaken this dependence would be desirable. Second, while the block implementation performs well empirically, a corresponding convergence theory remains to be developed. Finally, a refined finite-precision analysis could provide additional insight into rounding effects in practice especially when the matrix is ill-conditioned or has small gaps.

Acknowledgments. The authors thank Joel A. Tropp for suggesting to us the idea of using randomization to precondition a tall-skinny nullspace algorithm. We

also thank Chris Camaño and Raphael Meyer for helpful conversations.

REFERENCES

- [1] G. ABRAHAM AND M. INOUYE, *Fast principal component analysis of large-scale genome-wide data*, PloS one, 9 (2014), p. e93766, <https://doi.org/10.1371/journal.pone.0093766>. (Cited p. 1.)
- [2] F. ALIMISIS, D. KRESSNER, N. SHAO, AND B. VANDEREYCKEN, *A preconditioned inverse iteration with an improved convergence guarantee*, Numer. Math., (2026), <https://doi.org/10.1007/s00211-026-01525-7>. (Cited p. 5.)
- [3] A. ALLA AND J. N. KUTZ, *Randomized model order reduction*, Adv. Comput. Math., 45 (2019), pp. 1251–1271, <https://doi.org/10.1007/s10444-018-09655-9>. (Cited p. 1.)
- [4] M. E. ARGENTATI, A. V. KNYAZEV, K. NEYMEYR, E. E. OVTCHINNIKOV, AND M. ZHOU, *Convergence theory for preconditioned eigenvalue solvers in a nutshell*, Found. Comput. Math., 17 (2017), pp. 713–727, <https://doi.org/10.1007/s10208-015-9297-1>. (Cited p. 5.)
- [5] H. AVRON, P. MAYMOUNKOV, AND S. TOLEDO, *Blendenpik: Supercharging LAPACK’s least-squares solver*, SIAM J. Sci. Comp., 32 (2010), pp. 1217–1236, <https://doi.org/10.1137/090767911>. (Cited p. 1.)
- [6] K. BATSELIER, P. DREESEN, AND B. DE MOOR, *On the null spaces of the Macaulay matrix*, Linear Algebra Appl., 460 (2014), pp. 259–289, <https://doi.org/10.1016/j.laa.2014.07.035>. (Cited p. 1.)
- [7] C. CAMAÑO, E. N. EPPERLY, R. A. MEYER, AND J. A. TROPP, *Faster linear algebra algorithms with structured random matrices*, arXiv preprint [arXiv:2508.21189](https://arxiv.org/abs/2508.21189), (2025). (Cited p. 7.)
- [8] T. CHEN, E. N. EPPERLY, R. A. MEYER, C. MUSCO, AND A. RAO, *Does block size matter in randomized block Krylov low-rank approximation?*, in Proceedings of the 2026 Annual ACM-SIAM Symposium on Discrete Algorithms (SODA), SIAM, 2026, <https://doi.org/10.1137/1.9781611978971.42>. (Cited p. 14.)
- [9] S. CHENAKKOD, M. DEREZIŃSKI, AND X. DONG, *Optimal oblivious subspace embeddings with near-optimal sparsity*, in Proceedings of the 52nd International Colloquium on Automata, Languages, and Programming (ICALP), 2025, <https://doi.org/10.4230/LIPIcs.ICALP.2025.55>. (Cited p. 7.)
- [10] S. CHENAKKOD, M. DEREZIŃSKI, AND X. DONG, *Optimal subspace embeddings: Resolving Nelson-Nguyen conjecture up to sub-polylogarithmic factors*, in Proceedings of the 2026 Annual ACM-SIAM Symposium on Discrete Algorithms (SODA), SIAM, 2026, <https://doi.org/10.1137/1.9781611978971.163>. (Cited p. 7.)
- [11] M. B. COHEN, *Nearly tight oblivious subspace embeddings by trace inequalities*, in Proceedings of the Twenty-Seventh Annual ACM-SIAM Symposium on Discrete Algorithms (SODA), SIAM, January 2016, pp. 278–287, <https://doi.org/10.1137/1.9781611974331.ch21>. (Cited p. 7.)
- [12] C. DAVIS AND W. M. KAHAN, *The rotation of eigenvectors by a perturbation. III*, SIAM J. Numer. Anal., 7 (1970), pp. 1–46, <https://doi.org/10.1137/0707001>. (Cited p. 12.)
- [13] Y. DONG AND P.-G. MARTINSSON, *Simpler is better: A comparative study of randomized pivoting algorithms for CUR and interpolative decompositions*, Adv. Comput. Math., 49 (2023), p. 66, <https://doi.org/10.1007/s10444-023-10061-z>. (Cited p. 7.)
- [14] T. A. DRISCOLL, Y. NAKATSUKASA, AND L. N. TREFETHEN, *AAA rational approximation on a continuum*, SIAM J. Sci. Comp., 46 (2024), pp. A929–A952, <https://doi.org/10.1137/23M1570508>. (Cited p. 16.)
- [15] J. A. DUERSCH, M. SHAO, C. YANG, AND M. GU, *A robust and efficient implementation of LOBPCG*, SIAM J. Sci. Comp., 40 (2018), pp. C655–C676, <https://doi.org/10.1137/17M1129830>. (Cited pp. 5 and 6.)
- [16] E. N. EPPERLY, *Make the Most of What You Have: Resource-efficient Randomized Algorithms for Matrix Computations*, PhD thesis, California Institute of Technology, 2025. (Cited p. 7.)
- [17] A. C. GILBERT, J. Y. PARK, AND M. B. WAKIN, *Sketched SVD: Recovering spectral features from compressive measurements*, arXiv preprint [arXiv:1211.0361v1](https://arxiv.org/abs/1211.0361v1), (2012). (Cited p. 9.)
- [18] G. H. GOLUB AND C. F. VAN LOAN, *An analysis of the total least squares problem*, SIAM J. Numer. Anal., 17 (1980), pp. 883–893, <https://doi.org/10.1137/0717073>. (Cited p. 1.)
- [19] G. H. GOLUB AND C. F. VAN LOAN, *Matrix Computations*, Johns Hopkins Studies in the Mathematical Sciences, Johns Hopkins Press, Baltimore, fourth ed., 2013. (Cited p. 2.)
- [20] N. GOVINDARAJAN, R. WIDDERSHOVEN, S. CHANDRASEKARAN, AND L. DE LATHAUWER, *A fast algorithm for computing Macaulay null spaces of bivariate polynomial systems*, SIAM Jour-

- nal on Matrix Analysis and Applications, 45 (2024), pp. 368–396, <https://doi.org/10.1137/23M1550414>. (Cited p. 1.)
- [21] U. HETMANIUK AND R. LEHOUCQ, *Basis selection in LOBPCG*, Journal of Computational Physics, 218 (2006), pp. 324–332, <https://doi.org/10.1016/j.jcp.2006.02.007>. (Cited p. 5.)
- [22] A. KIREEVA AND J. A. TROPP, *Randomized matrix computations: Themes and variations*, (2024), <https://doi.org/10.7907/7yade-5k351>. (Cited pp. 3, 8, and 9.)
- [23] A. V. KNYAZEV, *Toward the optimal preconditioned eigensolver: Locally optimal block preconditioned conjugate gradient method*, SIAM J. Sci. Comp., 23 (2001), pp. 517–541, <https://doi.org/10.1137/S1064827500366124>. (Cited pp. 1, 6, and 8.)
- [24] A. V. KNYAZEV, M. E. ARGENTATI, I. LASHUK, AND E. E. OVTCHINNIKOV, *Block locally optimal preconditioned eigenvalue solvers (BLOPEX) in Hypre and PETSc*, SIAM J. Sci. Comp., 29 (2007), pp. 2224–2239, <https://doi.org/10.1137/060661624>. (Cited p. 8.)
- [25] A. V. KNYAZEV AND K. NEYMEYR, *A geometric theory for preconditioned inverse iteration III: A short and sharp convergence estimate for generalized eigenvalue problems*, Linear Algebra Appl., 358 (2003), pp. 95–114, [https://doi.org/10.1016/S0024-3795\(01\)00461-X](https://doi.org/10.1016/S0024-3795(01)00461-X). (Cited p. 5.)
- [26] D. KRESSNER AND N. SHAO, *A randomized small-block Lanczos method for large-scale null space computations*, arXiv preprint [arXiv:2407.04634v2](https://arxiv.org/abs/2407.04634v2), (2024). (Cited p. 1.)
- [27] P.-G. MARTINSSON AND J. A. TROPP, *Randomized numerical linear algebra: Foundations and algorithms*, Acta Numerica, 29 (2020), pp. 403–572, <https://doi.org/10.1017/S0962492920000021>. (Cited p. 7.)
- [28] R. MURRAY, J. DEMMEL, M. W. MAHONEY, N. B. ERICHSON, M. MELNICHENKO, O. A. MALIK, L. GRIGORI, P. LUSZCZEK, M. DEREZIŃSKI, M. E. LOPES, T. LIANG, H. LUO, AND J. DONGARRA, *Randomized numerical linear algebra: A perspective on the field with an eye to software*, arXiv preprint [arXiv:2302.11474v2](https://arxiv.org/abs/2302.11474v2), (2023). (Cited p. 7.)
- [29] Y. NAKATSUKASA, *Accuracy of singular vectors obtained by projection-based SVD methods*, BIT Numer. Math., 57 (2017), pp. 1137–1152, <https://doi.org/10.1007/s10543-017-0665-x>. (Cited p. 7.)
- [30] Y. NAKATSUKASA, *Sharp error bounds for Ritz vectors and approximate singular vectors*, Math. Comp., 89 (2020), pp. 1843–1866, <https://doi.org/10.1090/mcom/3519>. (Cited p. 7.)
- [31] Y. NAKATSUKASA, O. SÈTE, AND L. N. TREFETHEN, *The AAA algorithm for rational approximation*, SIAM J. Sci. Comp., 40 (2018), pp. A1494–A1522, <https://doi.org/10.1137/16M1106122>. (Cited pp. 1 and 16.)
- [32] Y. NAKATSUKASA AND L. N. TREFETHEN, *An algorithm for real and complex rational minimax approximation*, SIAM J. Sci. Comp., 42 (2020), pp. A3157–A3179, <https://doi.org/10.1137/19M1281897>. (Cited pp. 1 and 16.)
- [33] K. NEYMEYR, *A geometric theory for preconditioned inverse iteration I: Extrema of the Rayleigh quotient*, Linear Algebra Appl., 322 (2001), pp. 61–85, [https://doi.org/10.1016/S0024-3795\(00\)00239-1](https://doi.org/10.1016/S0024-3795(00)00239-1). (Cited p. 9.)
- [34] K. NEYMEYR, *A geometric convergence theory for the preconditioned steepest descent iteration*, SIAM J. Numer. Anal., 50 (2012), pp. 3188–3207, <https://doi.org/10.1137/11084488X>. (Cited pp. 5 and 9.)
- [35] E. OVTCHINNIKOV, *Cluster robustness of preconditioned gradient subspace iteration eigensolvers*, Linear Algebra Appl., 415 (2006), pp. 140–166, <https://doi.org/10.1016/j.laa.2005.06.039>. Special Issue on Large Scale Linear and Nonlinear Eigenvalue Problems. (Cited pp. 5 and 7.)
- [36] T. PARK AND Y. NAKATSUKASA, *A fast randomized algorithm for computing an approximate null space*, BIT Numer. Math., 63 (2023), p. 36, <https://doi.org/10.1007/s10543-023-00979-7>. (Cited pp. 2, 7, and 9.)
- [37] V. ROKHLIN, A. SZLAM, AND M. TYGERT, *A randomized algorithm for principal component analysis*, SIAM J. Matrix Anal. Appl., 31 (2010), pp. 1100–1124, <https://doi.org/10.1137/080736417>. (Cited p. 14.)
- [38] V. ROKHLIN AND M. TYGERT, *A fast randomized algorithm for overdetermined linear least-squares regression*, Proc. Natl. Acad. Sci. U. S. A., 105 (2008), pp. 13212–13217, <https://doi.org/10.1073/pnas.0804869105>. (Cited pp. 1 and 8.)
- [39] T. SARLÓS, *Improved approximation algorithms for large matrices via random projections*, in 2006 47th Annual IEEE Symposium on Foundations of Computer Science (FOCS), October 2006, pp. 143–152, <https://doi.org/10.1109/FOCS.2006.37>. (Cited p. 3.)
- [40] R. SCHMIDT, *Multiple emitter location and signal parameter estimation*, IEEE T Antenn Propag., 34 (1986), pp. 276–280, <https://doi.org/10.1109/TAP.1986.1143830>. (Cited p. 1.)
- [41] A. STATHOPOULOS AND K. WU, *A block orthogonalization procedure with constant synchronization requirements*, SIAM J. Sci. Comp., 23 (2002), pp. 2165–2182, <https://doi.org/10.1137/S1064827500366124>. (Cited p. 1.)

- 1137/S1064827500370883. (Cited p. 5.)
- [42] L. N. TREFETHEN, *Rational Chebyshev approximation on the unit disk*, Numer. Math., 37 (1981), pp. 297–320, <https://doi.org/10.1007/BF01398258>. (Cited p. 16.)
- [43] L. N. TREFETHEN, *Approximation Theory and Approximation Practice, Extended Edition*, SIAM, 2019, <https://doi.org/10.1137/1.9781611975949>. (Cited p. 16.)
- [44] J. A. TROPP, *Comparison theorems for the minimum eigenvalue of a random positive-semidefinite matrix*, arXiv preprint [arXiv:2501.16578](https://arxiv.org/abs/2501.16578), (2025). (Cited p. 7.)
- [45] J. A. TROPP AND R. J. WEBBER, *Randomized algorithms for low-rank matrix approximation: Design, analysis, and applications*, arXiv preprint [arXiv:arXiv:2306.12418v3](https://arxiv.org/abs/2306.12418v3), (2023). (Cited p. 14.)
- [46] J. A. TROPP, A. YURTSEVER, M. UDELL, AND V. CEVHER, *Streaming low-rank matrix approximation with an application to scientific simulation*, SIAM J. Sci. Comp., 41 (2019), pp. A2430–A2463, <https://doi.org/10.1137/18M1201068>. (Cited p. 1.)
- [47] P.-Å. WEDIN, *Perturbation bounds in connection with singular value decomposition*, BIT Numer. Math., 12 (1972), pp. 99–111, <https://doi.org/10.1007/BF01932678>. (Cited p. 12.)
- [48] L. WU AND A. STATHOPOULOS, *A preconditioned hybrid SVD method for accurately computing singular triplets of large matrices*, SIAM J. Sci. Comp., 37 (2015), pp. S365–S388, <https://doi.org/10.1137/140979381>. (Cited p. 13.)
- [49] M. ZHOU, A. KNYAZEV, AND K. NEYMEYR, *Angle-free cluster-robust Ritz value bounds for restarted block eigensolvers*, Numer. Linear Algebra Appl., 32 (2025), p. e2607, <https://doi.org/10.1002/nla.2607>. (Cited p. 7.)